

5-1-2002

## Zero-bias anomaly in CrO<sub>2</sub> junctions

Andrei Sokolov

*University of Nebraska-Lincoln, sokolov@unl.edu*

C.-S. Yang

*University of Nebraska - Lincoln*

Lu Yuan

*Physics Department, University of Nebraska, lyuan2@bigred.unl.edu*

Sy\_Hwang Liou

*University of Nebraska-Lincoln, sliou@unl.edu*

Ruihua Cheng

*University of Nebraska - Lincoln*

*See next page for additional authors*

Follow this and additional works at: <http://digitalcommons.unl.edu/physicsdowben>

 Part of the [Physics Commons](#)

---

Sokolov, Andrei; Yang, C.-S.; Yuan, Lu; Liou, Sy\_Hwang; Cheng, Ruihua; Jeong, H.-K.; Komesu, T.; Xu, B.; Borca, C.N.; Dowben, Peter A.; and Doudin, Bernard, "Zero-bias anomaly in CrO<sub>2</sub> junctions" (2002). *Peter Dowben Publications*. 92.

<http://digitalcommons.unl.edu/physicsdowben/92>

This Article is brought to you for free and open access by the Research Papers in Physics and Astronomy at DigitalCommons@University of Nebraska - Lincoln. It has been accepted for inclusion in Peter Dowben Publications by an authorized administrator of DigitalCommons@University of Nebraska - Lincoln.

---

**Authors**

Andrei Sokolov, C.-S. Yang, Lu Yuan, Sy\_Hwang Liou, Ruihua Cheng, H.-K. Jeong, T. Komesu, B. Xu, C.N. Borca, Peter A. Dowben, and Bernard Doudin

## Zero-bias anomaly in CrO<sub>2</sub> junctions

A. SOKOLOV, C.-S. YANG, L. YUAN, S.-H. LIOU, RUIHUA CHENG, H.-K. JEONG, T. KOMESU, B. XU, C. N. BORCA, P. A. DOWBEN and B. DOUDIN

*Center for Materials Research and Analysis and Department of Physics and Astronomy Behlen Laboratory of Physics, University of Nebraska - Lincoln, NE 68588-0111, USA*

(received 12 October 2001; accepted in final form 5 February 2002)

PACS. 75.70.-i – Magnetic properties of thin films, surfaces, and interfaces.

PACS. 81.15.Gh – Chemical vapor deposition (including plasma-enhanced CVD, MOCVD, etc.).

PACS. 82.30.Lp – Decomposition reactions (pyrolysis, dissociation, and fragmentation).

**Abstract.** – CrO<sub>2</sub> thin films, with crystallites of several microns size, provide the opportunity for the investigation of the intergrain tunneling between a few crystals separated by a 1–2 nm thick Cr<sub>2</sub>O<sub>3</sub> film. A pronounced zero-bias anomaly of the conductance is found at low temperatures. Combined photoemission and inverse photoemission temperature-dependent studies confirm the occurrence of Coulomb blockade. For the strong-tunneling case ( $R \ll R_Q = h/2e^2$ ), the magnetoresistance decreases strongly with bias. For the weak-tunneling case ( $R \gg R_Q$ ), the magnetoresistance decreases by a factor two with increasing bias, as predicted by a co-tunneling model.

One of the most desirable properties of a ferromagnetic material for spintronics applications is a high degree of polarization of the conduction electron spins. This has motivated investigation of half-Heusler alloys (NiMnSb), colossal magnetoresistance materials (La<sub>1-x</sub>Sr<sub>x</sub>MnO<sub>3</sub>), and semi-metal magnetic oxides (CrO<sub>2</sub>, Fe<sub>3</sub>O<sub>4</sub>) for evidence of 100% spin polarization. CrO<sub>2</sub> pressed powders and CrO<sub>2</sub>/Cr<sub>2</sub>O<sub>3</sub> composites showed a remarkable magnetoresistance (MR) of up to 50% at low temperature, with the magnetoresistance decreasing rapidly with increasing temperature [1–3]. The results were explained in terms of intergrain tunneling, and the large MR values were attributed to the high degree of spin polarization of CrO<sub>2</sub>. Evidence of the large spin polarization for CrO<sub>2</sub> has been suggested by superconducting point contact spectroscopy [4], but some care must be taken when comparing these results with spin polarization of tunneling electrons [5]. Additional evidence of high values of polarization has been found by spin-polarized photoemission [6] and vacuum tunneling [7], but the interpretation of these latter results needs to take into account the limited wave vector sampling and strong surface effects. Very large MR ratios are expected for tunnel junctions made of high spin polarization materials, however, only a very small MR ratio (1%) at 70 K [8], or even negative MR (–8%) at 4.2 K [9] have been observed. There is a clear need of clarification of the electric transport in chromium oxide junctions, as well as understanding the decrease of MR when increasing the temperature. For applications, reproducible and optimized MR values are necessary.

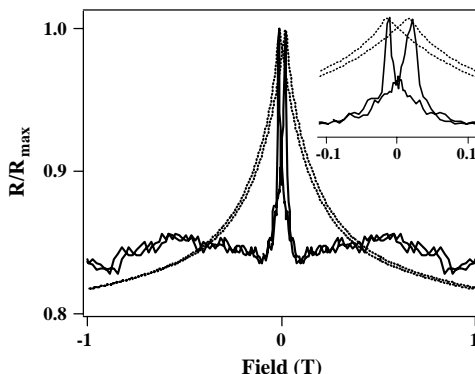


Fig. 1 – Magnetoresistance curve at 3 K of a chromium oxide thin film with an electric percolation path through a few (typically 10) CrO<sub>2</sub> crystallites. The dotted curve is a measurement performed on a low-resistance chromium oxide thick film, where the percolation path goes through many (estimated larger than 100) crystallites.

In this letter, we report the results on samples made of large crystallites. This allowed us to make electrical connections to a small number of crystals. Our measurements provide evidence of the importance of the so-called “zero-bias anomaly”, indicated by a strong non-linearity of the  $IV$  curves at low voltage bias [10]. We show that the observed MR is closely related to this anomaly and may be explained in terms of Coulomb blockade. Our data supports a model of MR governed by spin blockade effects, disappearing when thermal fluctuations overcome the blockade energy. Photoemission and inverse photoemission studies confirm this hypothesis in illustrating a remarkable decrease of the conduction-band edge energy with increasing temperatures. We have already confirmed the presence of a Cr<sub>2</sub>O<sub>3</sub> insulating oxide at the surface [11], consistent with Dai *et al.* [12] findings on commercial CrO<sub>2</sub> powders. Impurities in the insulating oxide are our best candidates for blocking the electric transport in our junctions. We compare our results to the theoretical models of enhancements of the MR due to spin blockade effects. At low voltage bias, the MR value is twice the value at large bias, in accordance with the predictions from a model of co-tunneling of Takahashi and Maekawa [13]. Cases where the MR ratio decreases strongly with voltage bias are explained by a lower intergrain resistance of the samples, where quantum fluctuations cannot be neglected.

Polycrystalline CrO<sub>2</sub> films were made by RF sputtering of CrO<sub>3</sub> onto LaAlO<sub>3</sub> substrates and annealing in a high-pressure cell. The sputtering was performed under 10 mTorr argon and 2 mTorr oxygen pressure. The target was prepared by pressing CrO<sub>3</sub> powder and sintering at 150 °C. The thickness of the CrO<sub>2</sub>/CrO<sub>3</sub> films ranged between 0.1 μm and 1 μm. Annealing in about 100 atms of oxygen pressure at 390 °C leads to a stable CrO<sub>2</sub> phase [1, 14]. X-ray diffraction confirmed the presence of CrO<sub>2</sub> with no detectable diffraction peaks from Cr<sub>2</sub>O<sub>3</sub>. The thinnest annealed films showed a grain density of about 10 crystals every 100 μm<sup>2</sup> area. The grains were of elongated shape, typically 5 μm long and 0.5 μm wide, as revealed by SEM and AFM observations.

The surface composition of our samples was investigated by angle-resolved X-ray photoemission (XPS), revealing a Cr<sub>2</sub>O<sub>3</sub> coverage of 1–2 nm thick [11]. It is known that Cr<sub>2</sub>O<sub>3</sub> is thermodynamically more stable than CrO<sub>2</sub> [1, 15] and is the generally accepted stable surface of CrO<sub>2</sub> [12]. This insulating surface oxide also plays the role of a thin tunnel barrier between adjacent crystallites. Electric measurements were performed on thin, non-continuous CrO<sub>2</sub> films. Samples were not patterned, on substrates typically 0.5 mm × 3 mm large. Silver

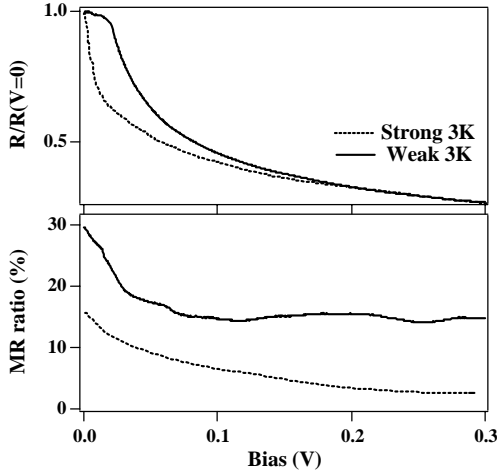


Fig. 2

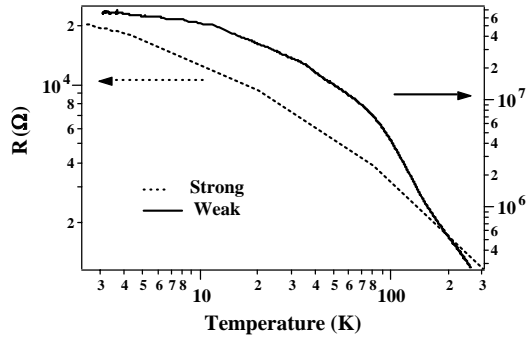


Fig. 3

Fig. 2 – Top: normalized resistance as a function of voltage bias for two types of samples made of 10–20 junctions in series. The weak-tunneling sample (—) has a resistance of more than  $40R_Q$  (at 0.5 V bias). The strong-tunneling case (....) corresponds to a sample of resistance smaller than  $0.5R_Q$  (at 0.5 V bias). Bottom: magnetoresistance as a function of voltage bias. For the weak-tunneling sample, it decreases by a factor two with increasing bias (co-tunneling model). For the strong-tunneling case, the decrease as a function of bias is more pronounced down to MR values of a few percents only.

Fig. 3 – Zero-bias conductance as a function of temperature (1 mV rms excitation, measured at 100 Hz).

epoxy glued connections were separated by less than  $200 \mu\text{m}$ . Comparison between 2 and 4 points measurements indicated that the contact resistance was not exceeding a few ohms, on samples of several  $\text{k}\Omega$  resistance. A typical MR curve is shown in fig. 1. The maximum ( $R_{\text{max}}$ ) of the MR curve corresponds to the zero total magnetization of the film, where the probability of anti-parallel alignment of neighbor crystallites is highest. Applied fields larger than 0.1 T saturate the MR and the magnetization of our samples. The MR ratio, defined as  $(R_{\text{max}} - R)/R_{\text{max}}$ , had values of typically 15% to 25%. The MR ratio decreases exponentially with increasing temperature to values lower than 1% at temperatures higher than 100 K. This is consistent with the results observed on  $\text{CrO}_2$  powders [1–3].

Studies on samples made of a few crystals allow us to characterize the non-linear  $\text{CrO}_2$  intergrain conductivity, which includes  $\text{Cr}_2\text{O}_3$  barrier layers, without resorting to the investigation of the  $\text{CrO}_2/\text{Cr}_2\text{O}_3$  composite system. Resistance curves revealed strong non-linear characteristics at low bias (fig. 2). The large-bias (more than 0.5 V) current is still slightly non-linear, but does not vary significantly with temperature. A basic approximation for a tunnel junction predicts a temperature-independent parabolic conductance-voltage curve. This describes the high-bias conductance behavior of our samples. For comparison purposes, the same measurements were performed on thick-films samples, of typical resistance of a few ohms, made of hundreds of connections (between  $\text{CrO}_2$  grains) in series and parallel. A bias of 1 V corresponds to sub-mV bias for an individual junction. Such samples showed less than 1% change in conductance within 1 V bias range. These samples also show MR curves (fig. 1), with the only difference being the higher magnetic fields needed to saturate the resistance, as observed by others [1, 2].

The low-bias conductivity is strongly reminiscent of the so-called “giant resistance peak” observed by Rowell and Shen on Cr-I-Ag tunnel junctions [16]. This insulator “I” was fabricated by oxidation of a Cr film, and the anomaly attributed to the presence of magnetic CrO<sub>2</sub> and Cr<sub>2</sub>O<sub>3</sub>! The half-width of the giant resistance peak we found at 3 K is between 50 mV and 75 mV, which are 10–15 times larger than Rowell and Shen results (fig. 1 in [16]). Our data presented in fig. 2 (top) corresponds directly to the Rowell and Shen results if we scale down our bias voltage scale by a factor 10–15. We can therefore infer that our samples are made of a limited number of junctions in series (10–15). The two curves shown in fig. 2 (top) have different scaling factors, a consequence of the two samples having a different number of junctions in series. Explanations for the giant resistance peak were given by Giaver and Zeller in their seminal paper on Coulomb blockade in tunnel junctions [17]. The low-bias peak corresponds to the current blocking due to the electrostatic charging energy of an island within the tunnel junction barrier. The magnitude of the Coulomb blockade can be estimated from the width (5 mV) of the resistance peak found by Rowell and Shen [16]. Blockade energies in the region of 5–20 meV can be deduced from our data, though large uncertainties exist due to the increase of resistance peak width with temperature [16].

The interplay between Coulomb blockade and tunnel magnetoresistance (TMR) has recently attracted a lot of interest, mostly motivated by the perspective of the TMR enhancement by spin blockade effects. Theoretical models involving co-tunneling [13] and spin accumulation [18,19] have been put forward. Figure 2 (bottom) shows how the MR diminishes with voltage bias. The magnetoresistance behavior corresponds to the predictions of Takahashi and Maekawa model of enhancement of MR due to co-tunneling effects [13]. The Coulomb blockade electrostatic energy leads to an exponential increase in the resistance at low temperatures in a sequential tunneling model. Averin and Nazarov [20] showed that inelastic co-tunneling, where the electrons tunnel through a virtual state in an island within the dielectric barrier, becomes a dominant current path at low temperatures and low bias. This co-tunneling event has a probability proportional to the product of the probability to add an electron to the island with the escape probability of an electron out of the island. The MR ratio for such fully correlated events is therefore twice the MR ratio of uncorrelated events, or sequential tunneling, occurring at high-voltage bias. Our data confirmed this prediction for samples of high resistance (several hundreds of kΩ at room temperature), where changes in the annealing parameters allowed us to increase the Cr<sub>2</sub>O<sub>3</sub> barrier thickness [1]. Figure 2 indicates that a low-bias MR of 30% decreases down 15% at higher bias. This reduction by a factor two is following the co-tunneling model predictions. For lower-resistance samples (a few kΩ at room temperature), much lower MR values at high bias are observed. This difference is explained in terms of quantum fluctuations. For the low-resistance samples, the intergrain resistance is much smaller than the quantum of resistance ( $R_Q = h/2e^2 \approx 13.8 \text{ k}\Omega$ ), which is classified as strong-tunnel regime. The MR at large bias becomes much smaller (down to a few percent, fig. 2), in agreement with theoretical predictions [13, 21]. In view of applications of TMR for devices, our data indicate that lowering the barrier resistance (needed for application in sensors) is at the expense of the bias dependence of the MR values.

The relative temperature variation of the zero-bias resistance was found to be similar for all samples (fig. 3). The data for Rowell and Shen superimposes to the data shown for strong-tunneling samples, as well as samples of resistance down a few tens of ohms. This is quite remarkable, when we keep in mind that our samples had resistance values spans of six orders of magnitude. The co-tunneling model predicts a quadratic variation of the resistance with temperature, becoming linear when the sequential tunneling becomes dominant at higher temperatures ( $k_B T > 0.1 E_c$ ) [13]. A linear behavior in the temperature range 50–200 K and a quadratic variation in the temperature range 10–50 K can be inferred from the data, but the

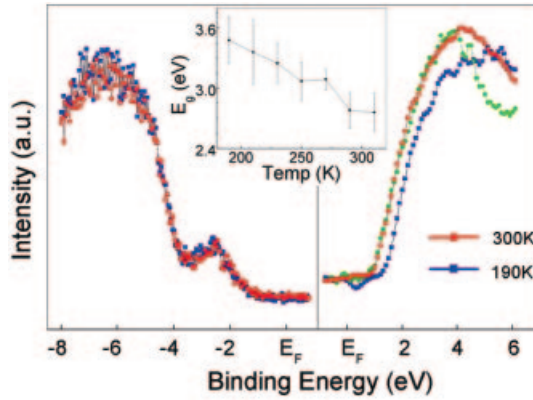


Fig. 4 – Photoemission spectrum (left) and inverse photoemission spectrum (right) of the  $\text{Cr}_2\text{O}_3$  coverage of  $\text{CrO}_2$  crystallites, measured at 190 K (blue dots) and 300 K (red dots). The bandgap as a function of temperature, calculated from the combination of the two types of photoemission, is shown in the insert. The error bars are upper bound values summing the worst cases of the two techniques, and include a variety of systematic errors. No temperature shift of the conduction-edge band occur for the Ar ion sputtered surface, for which the spectrum measured at 190 K is shown (green dots).

observed saturation behavior seen at lower temperatures cannot be accounted for. Theoretical predictions exist however for explaining a saturation of the resistance in the strong-tunneling regime at low temperatures [21].

Photoemission and inverse photoemission measurements were used to confirm the occurrence of spin blockade effects. These surface characterization techniques, complementary to transport studies, allow us to discard a model where heating of the junctions is a source of strong non-linear resistance curves. Prior to photoemission experiments, appropriate surface preparation was established by XPS, ultraviolet photoemission and inverse photoemission. A negligible amount of  $C$  (less than 3% of a monolayer) was a good indicator of a clean surface following sputtering and annealing at 350 K. The electronic valence bands were acquired at normal emission with a He I incident radiation source (21.3 eV). The inverse photoemission spectra were obtained by using variable energy electron and UV detector (a Geiger-Müller detector). The instrument linewidth is  $\sim 400$  meV, and peak positions are calibrated with respect to the Fermi level established from tantalum in electrical contact with the sample for both photoemission and inverse photoemission with 50 meV accuracy. The conduction band spectra were taken by changing the kinetic energy of the incidence electron energy from 5 eV to 19 eV. Selected spectra are shown in fig. 4. At all temperatures investigated, the large gap ( $3.5 \pm 0.15$  eV at 190 K) confirms that the  $\text{Cr}_2\text{O}_3$  coverage of a  $\text{CrO}_2$  grain provides a wide band gap tunnel barrier. Heating the sample to room temperature showed a significant decrease of the conduction band edge energy, without other significant changes in the spectra. An unambiguous temperature-dependent change of the valence band to conduction band gap by 0.7 eV, with non-systematic error estimate of 0.15 eV, was found between 190 and 300 K. The presence of intermediate states for conduction electrons in the  $\text{Cr}_2\text{O}_3$  barrier at the surface of chromium oxide samples cannot be explained in terms of the intrinsic semiconductor properties, because the shift with temperature is much greater than  $3k_B T$ . The error on this shift is reduced by a factor two when taking onto account the inverse photoemission data only. Special care was taken to exclude surface charging effects. The photocurrents generated in XPS (several  $\mu\text{A}$ ) are far larger than the incident fluxes in inverse photoemis-

sion (100–200 nA). XPS data should therefore be more sensitive to surface charging effects. No detectable shifts of core-level peaks and no power dependence (fluence) on the binding energies were found, with the very thin Cr<sub>2</sub>O<sub>3</sub> overlayers. The hypothesis of surface phase transition is very unlikely as no changes in the spectrum and no discontinuity in the bandgap values were observed when varying the temperature. Finally, we found that under appropriate surface treatment by sputtering, the conduction band edge is temperature independent, and corresponding to the high-temperature edge of the initial sample (the green curve in fig. 4 was taken at 190 K). After such a surface treatment, core level photoemission provided no indication that the overlayer is still anything other than a Cr<sub>2</sub>O<sub>3</sub> overlayer on CrO<sub>2</sub>. The photoemission data therefore confirms that intermediate states in the bandgap of the native insulating Cr<sub>2</sub>O<sub>3</sub> layer become available when providing thermal energy of typically 10 meV to the system. This is the same energy range as the Coulomb blockade energy found by electric transport measurements.

We find conclusive evidence, through several different experimental techniques, that the spin transport in CrO<sub>2</sub> powders exhibits spin blockade properties at low temperatures. We provide compelling evidence, for the first time, that the transition between strong-tunneling and weak-tunneling regimes modifies significantly the MR properties, in accordance with the prediction of Takahashi and Maekawa [13]. For single CrO<sub>2</sub>/Cr<sub>2</sub>O<sub>3</sub> junctions, we find that a voltage bias of more than 5 mV is enough to drastically reduce the MR to very low values if the junction resistance is small (typically smaller than 10 kΩ). This, in addition to the above-noted temperature effects, might explain why such low MR ratio has been found on CrO<sub>2</sub> junctions [8]. The blockade energy estimates indicate that the size of the defects, within the barrier layers, has nothing to do with the size of the CrO<sub>2</sub> crystallites. The best candidates for intrinsic defects are off stoichiometry oxides at the CrO<sub>2</sub> and Cr<sub>2</sub>O<sub>3</sub> interface. Tunneling through impurities in tunnel junctions was predicted to cause a reversal of the sign of the MR ratio in some cases [22], as found on chromium oxide junctions [9]. With increasing temperature, we propose that the “Coulomb island” becomes a spin scattering center, diminishing further the MR ratio. Our measurements are also in agreement with past findings on Cr-I-Ag junctions, thus resolving a controversy for explaining such junctions in terms of Coulomb blockade [10]. Our results show that the large MR values found on CrO<sub>2</sub> are due to co-tunneling enhancement of the TMR ratio, and one does not need to take into account the expected large spin polarization of CrO<sub>2</sub> to explain such behavior. In the search for large tunnel magneto-resistive systems, alternatives to Cr<sub>2</sub>O<sub>3</sub> native oxide barriers must be found.

\* \* \*

The support of the NSF CAREER program (grant DMR 98-74657), the NSF (DMR 98-02126), the Office of Naval Research, and the Nebraska Research Initiative are gratefully acknowledged.

## REFERENCES

- [1] HWANG H. Y. and CHEONG S.-W., *Science*, **278** (1998) 1607.
- [2] COEY J. M. D., BERKOWITZ A. E., BALCELL S. L. and PUTRIS F. F., *Phys. Rev. Lett.*, **80** (1998) 3815.
- [3] MANOHARAN S. S., ELEFANT D., REISS G. and GOODENOUGH J. B., *Appl. Phys. Lett.*, **72** (1998) 984.
- [4] SOULEN R. J. *et al.*, *Science*, **282** (1998) 85.
- [5] MAZINI I. I., *Phys. Rev. Lett.*, **83** (1999) 1427.



- [6] KÄMPER K. P., SCHMITT W., GÜNTHERODT G., GAMBINO R. J. and RUF R., *Phys. Rev. Lett.*, **59** (1987) 2788.
- [7] WEISENDANGER R., GÜNTHERODT H.-J., GÜNTHERODT G., GAMBINO R. J. and RUF R., *Phys. Rev. Lett.*, **65** (1990) 247.
- [8] BARRY A., COEY J. M. D. and VIRET M., *J. Phys. Condens. Matter*, **12** (2000) L173.
- [9] GUPTA A. A., LI X. W. and XIAO G., *Appl. Phys. Lett.*, **78** (2001) 1894.
- [10] WOLF E. L., *Principles of Electron Tunneling Spectroscopy* (Oxford University Press) 1985.
- [11] CHENG R. *et al.*, *Appl. Phys. Lett.*, **79** (2001) 3122.
- [12] DAI J. *et al.*, *Appl. Phys. Lett.*, **77** (2000) 2840.
- [13] TAKAHASHI S. and MAEKAWA S., *Phys. Rev. Lett.*, **80** (1998) 1758.
- [14] CHAMBERLAND B. L., *CRC Crit. Rev. Solid State Mater. Sci.*, **7** (1977) 1.
- [15] ROBBERT P. S. *et al.*, *J. Vac. Sci. Technol. A*, **16** (1998) 990.
- [16] ROWELL J. M. and SHEN L. Y. L., *Phys. Rev. Lett.*, **17** (1966) 15.
- [17] GIAVER I. and ZELLER H. R., *Phys. Rev. Lett.*, **20** (1968) 1504.
- [18] BARNAS J. and FERT A., *Phys. Rev. Lett.*, **80** (1998) 1058.
- [19] BRATAAS A., NAZAROV Y. V., INOUE J. and BAUER G. E., *Phys. Rev. B*, **59** (1999) 93.
- [20] AVERIN D. V. and NAZAROV YU. V., *Phys. Rev. Lett.*, **65** (1990) 2446.
- [21] KONIG J., SCHOELLER H. and SCHON G., *Phys. Rev. Lett.*, **78** (1997) 4482.
- [22] TSYMBAL E. Y. and PETTIFOR D. G., *Phys. Rev. B*, **64** (2001) 212401.